PCCP

COMMUNICATION

View Article Online
View Journal | View Issue

Cite this: *Phys. Chem. Chem. Phys.*, 2017, **19**, 29760

Received 21st January 2017,
Accepted 30th October 2017

DOI: 10.1039/c7cp00474e

rsc.li/pccp

Electrophilicity of oxalic acid monomer is enhanced in the dimer by intermolecular proton transfer†

Zibo G. Keolopile, *[ab] Matthew R. Ryder, [ac] Benjamin Calzada,‡[a] Maciej Gutowski, *[a] Allyson M. Buytendyk,[d] Jacob D. Graham [d] and Kit H. Bowen*[d]

We have analyzed the effect of excess electron attachment on the network of hydrogen bonds in the oxalic acid dimer $(OA)_2$. The most stable anionic structures may be viewed as complexes of a neutral hydrogenated moiety HOA• coordinated to an anionic deprotonated moiety $(OA–H)^-$. HOA• acts as a double proton donor and $(OA–H)^-$ as a double proton acceptor. Thus the excess electron attachment drives intermolecular proton transfer. We have identified several cyclic hydrogen bonded structures of $(OA)_2^-$. Their stability has been analyzed in terms of the stability of the involved conformers, the energetic penalty for deformation of these conformers to the geometry of the dimer, and the two-body interaction energy between the deformed HOA• and $(OA–H)^-$. There are at least seven isomers of $(OA)_2^-$ with stabilization energies in the range of 1.26–1.39 eV. These energies are dominated by attractive two-body interaction energies. The anions are vertically bound electronically by 3.0–3.4 eV and adiabatically bound by at least 1.6 eV. The computational predictions are consistent with the anion photoelectron spectrum of $(OA)_2^-$. The spectrum consists of a broad feature, with an onset of 2.5 eV and spanning to 4.3 eV. The electron vertical detachment energy (VDE) is assigned to be 3.3 eV.

Introduction

Oxalic acid (OA) is the simplest dicarboxylic acid, see **N1** in Fig. 1, and can exist in several conformational forms differing in the extent of intramolecular hydrogen bonding. The clusters of OA are intriguing because of the competition between inter- and intramolecular hydrogen bonds. This phenomenon attracted the attention of many experimental[1–4] and computational[1,5–8] groups. The neutral dimer of oxalic acid, $(OA)_2$, has recently been studied computationally.[5,6] Many dimer structures are possible resulting from pairing miscellaneous conformers of OA through various sets of intermolecular hydrogen bonds. The structures with cyclic (double) hydrogen bonds were natural suspects for the global minimum. Notice that each monomer can engage a proton donor and a proton acceptor site from either the same or neighbouring carboxylic group(s). We concluded[6] that a "side-to-side" structure, labelled **ND1** in Fig. 2, is more stable by 61 meV than the "head-to-head" **ND3** structure, which is supported by a standard structural motif of hydrogen-bonded carboxylic groups (as in the formic acid (FA) dimer). The global stability of **ND1** resulted from a balancing act between a moderately attractive two-body interaction and small repulsive one-body terms. **ND3**, on the other hand, was characterized by the most attractive two-body term. However, repulsive one-body terms, which result from compromising two out of four intramolecular hydrogen bonds, limited its overall stability.

Our recent experimental and computational results demonstrated an unusual electrophilicity of the oxalic acid monomer.[1] OA^- is characterized by an adiabatic and vertical electron binding energy of 0.72 and 1.08 eV, respectively. The OA monomer may be viewed as a product of condensation of two FA molecules (with the release of H_2). It is well established that the FA monomer does not support a bound anionic state.[1] The unique electrophilicity of OA may result from the proximity of the carboxylic groups. Indeed, the SOMO of the anion is dominated by a bonding C–C interaction. In addition, intramolecular hydrogen bonds stabilize OA^-.[1]

Here we analyse the effect of excess electron attachment on the network of hydrogen bonds (intra- and intermolecular) in the oxalic acid dimer and we consider the anion of the FA dimer as a reference point. In our past study, we demonstrated that $(FA)_2^-$ undergoes intermolecular proton transfer and supports a valence anion with an electron vertical detachment energy (VDE) of 2.35 eV, but an adiabatic electron affinity (AEA) close

[a] *Institute of Chemical Sciences, School of Engineering and Physical Sciences, Heriot-Watt University, Edinburgh, Scotland, EH14 4AS, UK. E-mail: keolopilezg@ub.ac.bw, m.gutowski@hw.ac.uk*
[b] *Department of Physics, University of Botswana, Private Bag 0022, Gaborone, Botswana*
[c] *Department of Engineering Science, University of Oxford, Parks Road, Oxford OX1 3PJ, UK*
[d] *Department of Chemistry, Johns Hopkins University, Baltimore, MD 21218, USA. E-mail: kbowen@jhu.edu*

† Electronic supplementary information (ESI) available. See DOI: 10.1039/c7cp00474e

‡ On leave from Université Joseph Fourier, IUT1, Département Chimie, 39-41 Boulevard Gambetta, 38000 Grenoble, France.

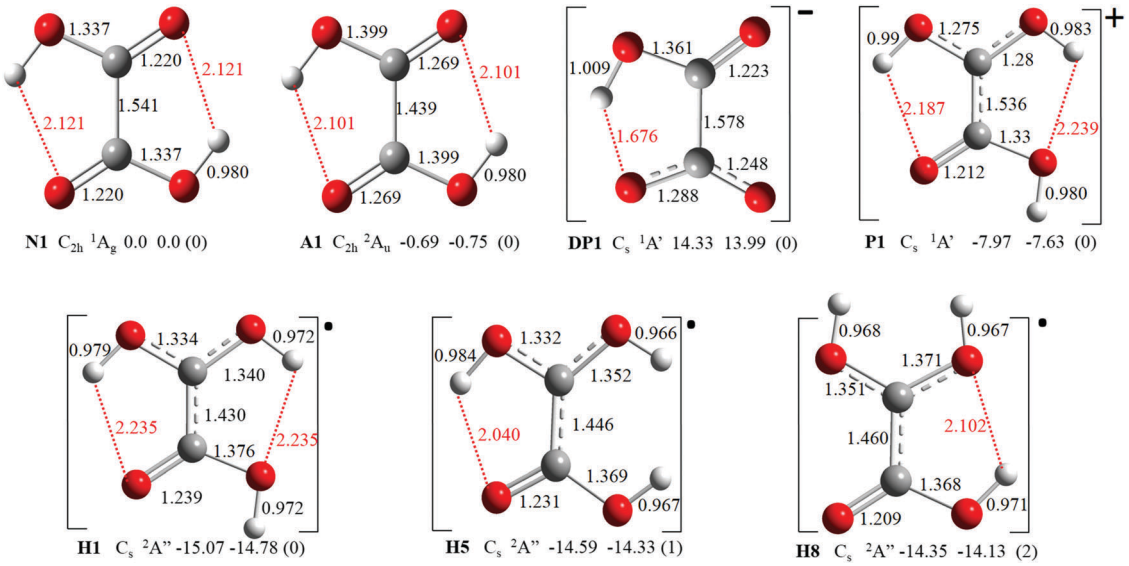

Fig. 1 Stationary points for the monomers of the neutral (**N**), anionic (**A**), deprotonated (**DP**), protonated (**P**), and hydrogenated (**H**) oxalic acid, which are relevant for the interpretation of results for $(OA)_2^-$. The name of the species is followed by its point symmetry group, the electronic term, two relative energies (in eV) with respect to **N1** (purely electronic and corrected for zero-point vibrations), and the number of vibrational modes with negative curvatures.

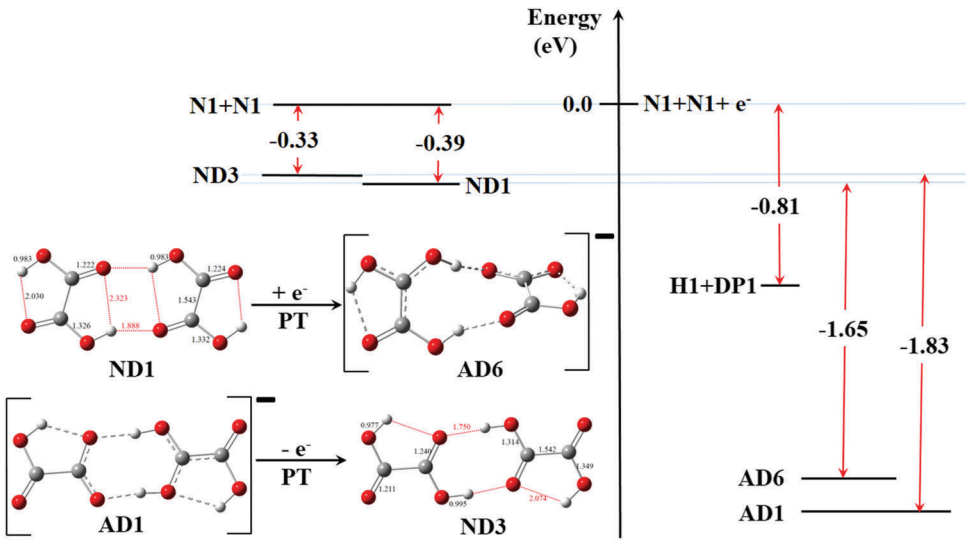

Fig. 2 Positions of the most stable neutral (**ND1**, left) and anionic (**AD1**, right) dimers with respect to their dissociative asymptotes. The energy of the **N1** + **N1** asymptote is set to zero. Evolution of **ND1** and **AD1** upon the excess electron attachment and detachment, respectively.

to zero ($|AEA| < 20$ meV).[9] The structure of the dimer anion resembles the formate anion engaged in a symmetrical double hydrogen-bonded bridge with the dihydroxymethyl radical. The relaxed anion of the FA dimer has now been experimentally characterized using Ar-tagged vibrational predissociation and electron autodetachment spectroscopies as well as anion photoelectron spectroscopy.[10] These results confirmed that the excess electron attachment leads to a transfer of one of the protons across the H-bonded bridge. The electron-induced proton transfer in the FA dimer is manifested also by differences in the results of electron energy-loss spectroscopy experiments on the monomer and dimer of FA.[11] The yield of very low energy electrons was found to be 20 times stronger in the dimer than in the monomer. The dramatic increase in the efficiency of the dimer to quasi-thermalize electrons arriving in the 1–2 eV energy range and captured in the lowest π^* shape resonance was interpreted in terms of a rapid intermolecular proton transfer that quenches the fast autodetachment channel.

In view of these results we suspected that the dimer of oxalic acid might also undergo intermolecular proton transfer upon excess electron attachment:

$$OA + OA \xrightarrow{+e} HOA^{\bullet}\cdots(OA{-}H)^-,$$

where $HOA^{\bullet}$ is a hydrogenated oxalic acid moiety (radical) and $(OA{-}H)^-$ is a deprotonated closed-shell moiety. For this reason,

we have analysed both the OA + OA^- and $HOA^\bullet$ + $(OA–H)^-$ asymptotes and we have discussed anionic dimers in terms of the interacting $HOA^\bullet$ and $(OA–H)^-$ moieties. The dimers have been found adiabatically bound and experimentally easily accessible. We conclude that the dimer of oxalic acid may serve as a model system for intermolecular proton transfer induced by a π excess electron.[12] Notice the role of proton motion coupled with electron transfer in bioenergetic conversion,[13] damage of nucleic acids by low-energy electrons,[14] protein redox machines,[15] and electron beam lithography.[16]

Methods

Here we apply a similar computational procedure to that of our study of the neutral oxalic acid dimer,[6] but adapted for excess charge and proton transfer. The most stable isomers of the anionic oxalic acid dimer might be viewed as an isomer *m* of the hydrogenated oxalic acid monomer $HOA^\bullet$, labelled **H*m***, interacting with an isomer *n* of the deprotonated monomer $(OA–H)^-$, labelled **DP*n***. **H*m***'s are neutral, doublet radicals and **DP*n***'s are negatively charged, closed-shell (singlet) moieties. The stability of the monomer decreases as *m* (or *n*) increases, with the most stable isomers being **H1** and **DP1**. For any geometry *G* of the anionic complex $HOA^\bullet\cdots(OA–H)^-$ we can identify an **H*m*** that resembles most the $HOA^\bullet$ monomer at the geometry *G*, *i.e.* $HOA^\bullet(G)$. An analogous procedure allows us to identify this **DP*n*** that resembles the most $(OA–H)^-(G)$. In consequence, we consider the $HOA^\bullet\cdots(OA–H)^-$ complex at the geometry *G* as a deformed **H*m*** interacting with a deformed **DP*n***, and we label this system as **H*m*DP*n***(*G*).

The total energy of $(OA)_2^-$ at a geometry *G* can be represented as:

$$E_{\mathrm{H}m\mathrm{DP}n}(G) = E_{\mathrm{H1}}(G_{\mathrm{H1}}) + E_{\mathrm{DP1}}(G_{\mathrm{DP1}}) + E^{\mathrm{stab}}_{\mathrm{H}m\mathrm{DP}n}(G), \quad (1)$$

where $E_{\mathrm{H1}}(G_{\mathrm{H1}})$ and $E_{\mathrm{DP1}}(G_{\mathrm{DP1}})$ are the energies of the most stable forms of $HOA^\bullet$ and $(OA–H)^-$, respectively, at their respective optimal geometries, and $E^{\mathrm{stab}}_{\mathrm{H}m\mathrm{DP}n}(G)$ is the stabilization energy calculated as:

$$E^{\mathrm{stab}}_{\mathrm{H}m\mathrm{DP}n}(G) = E^{\mathrm{1b}}_{\mathrm{H}m}(G) + E^{\mathrm{1b}}_{\mathrm{DP}n}(G) + E^{\mathrm{2b}}_{\mathrm{H}m\mathrm{DP}n}(G). \quad (2)$$

$E^{\mathrm{1b}}_{\mathrm{H}m}(G)$ is the one-body term defined as:

$$E^{\mathrm{1b}}_{\mathrm{H}m}(G) = E_{\mathrm{H}m}(G) - E_{\mathrm{H1}}(G_{\mathrm{H1}}), \quad (3)$$

where $E_{\mathrm{H}m}(G)$is the energy of $HOA^\bullet$ at the geometry *G*. $E^{\mathrm{1b}}_{\mathrm{H}m}(G)$ is the energy penalty for distorting the monomer $HOA^\bullet$ from the global minimum G_{H1} to the geometry *G*. The one body term $E^{\mathrm{1b}}_{\mathrm{H}m}(G)$ can be further split into a term that describes a conformational change from 1 to *m*, and the deformation from $G_{\mathrm{H}m}$ to *G*:

$$E^{\mathrm{1b}}_{\mathrm{H}m}(G) = E^{\mathrm{1b\text{-}conf}}_{1\to\mathrm{m}} + E^{\mathrm{1b\text{-}def}}_{\mathrm{H}m}(G), \quad (4)$$

with the conformation $E^{\mathrm{1b\text{-}conf}}_{1\to m}$ and deformation $E^{\mathrm{1b\text{-}def}}_{\mathrm{H}m}(G)$ penalties defined, respectively, as:

$$E^{\mathrm{1b\text{-}conf}}_{1\to m} = E_{\mathrm{H}m}(G_{\mathrm{H}m}) - E_{\mathrm{H1}}(G_{\mathrm{H1}}), \quad (5)$$

$$E^{\mathrm{1b\text{-}def}}_{\mathrm{H}m}(G) = E_{\mathrm{H}m}(G) - E_{\mathrm{H}m}(G_{\mathrm{H}m}). \quad (6)$$

Analogous definitions hold for the $E^{\mathrm{1b}}_{\mathrm{DP}n}(G)$ term. $E^{\mathrm{2b}}_{\mathrm{H}m\mathrm{DP}n}(G)$ is the two-body interaction energy calculated as:

$$E^{\mathrm{2b}}_{\mathrm{H}m\mathrm{DP}n}(G) = E_{\mathrm{H}m\mathrm{DP}n}(G) - E_{\mathrm{H}m}(G) - E_{\mathrm{DP}n}(G). \quad (7)$$

The total energy of the dimer is referenced with respect to the energies of the most stable isomers of $HOA^\bullet$ and $(OA–H)^-$, *i.e.*, **H1** and **DP1**; see eqn (1). Thus, $E^{\mathrm{stab}}_{\mathrm{H}m\mathrm{DP}n}(G)$ is a measure of the stability of the anionic complex at the geometry *G*.

The next, practical step is to determine the values of $E^{\mathrm{stab}}_{\mathrm{H}m\mathrm{DP}n}(G)$ as accurately as possible. When solving the electronic Schrödinger equation, one faces the challenges of electron correlation and incompleteness of the one-electron basis set. The approach we adopted here to obtain accurate electronic energies had been developed by the group of Hobza.[17] The geometries of the isolated monomers of the neutral (**N*n***), anionic (**A*n***), hydrogenated (**H*n***), deprotonated (**DP*n***), and protonated (**P*n***) OA, and of the neutral (**ND*n***) and anionic (**AD*n***) dimers of OA, were optimized at the MP2 level of theory[18] using the aug-cc-pVDZ[19] basis set. The single point energies of the monomers and dimers were extrapolated to the complete basis set (CBS) limit at the SCF and MP2 levels of theory using the aug-cc-pVNZ[19] basis sets (N = D, T, and Q). For the details of the extrapolation procedure see ref. 6. Higher-order electron correlation effects were estimated by performing single-point calculations at the CCSD(T) level of theory[20] using the aug-cc-pVDZ basis set. The incremental electron correlation energies were added to the sum of the CBS SCF and MP2-correlation terms to obtain our final electronic energies. Harmonic frequencies and zero-point vibrational corrections were obtained at the MP2 level using the aug-cc-pVDZ basis set.

The energies of the neutral and anionic dimers are contaminated with the so-called basis set superposition error, which distorts the equilibrium geometries and frequencies, as well as the values of $E^{\mathrm{stab}}_{\mathrm{H}m\mathrm{DP}n}(G)$.[21,22] The standard counterpoise (CP) procedure[23] was invoked when optimizing geometries and calculating vibrational frequencies of the anionic and neutral dimers, with the monomers $HOA^\bullet$ and $(OA–H)^-$ for the former and 2× OA for the latter. We also invoked the CP procedure to calculate the VDE and AEA values. The CBS-extrapolated dimer energies have been derived from the CP-corrected finite bases set energies.

All calculations were performed using the Gaussian 09 suite of programmes.[24] Molecular structures and orbitals were drawn using GaussView.[25] The contour values used in the plots were calculated with the OpenCubMan tool[26] using a fraction of electron density equal to 0.8. The Gaussian cube file was produced with a fine grid of 12 points per bohr.

On the experimental side, anion photoelectron spectroscopy was conducted by crossing a mass-selected beam of negative ions with a fixed-frequency photon beam and energy-analysing the resultant photodetached electrons. Photodetachment transitions occur between the ground state of a mass-selected negative ion and the ground and energetically accessible excited states of its neutral counterpart. This process is governed by the energy-conserving relationship $h\nu$ = EBE + EKE, where $h\nu$ is the photon

energy, EBE is the electron binding energy, and EKE is the electron kinetic energy. Measuring electron kinetic energies and knowing the photon energy provide electron binding (photodetachment transition) energies. Because these are vertical transitions, their relative intensities are determined by the extent of Franck–Condon overlap between the anion and its corresponding neutral. Our apparatus consists of a laser photoemission anion source, a linear time-of-flight mass spectrometer for mass analysis and mass selection, a momentum decelerator, a magnetic bottle electron energy analyzer, and a Nd:YAG photodetachment laser. The magnetic bottle has a resolution of ~50 meV at an EKE of 1 eV. In these experiments, photoelectron spectra were recorded with 266 nm (4.66 eV) photons. The photoelectron spectra were calibrated against the well-known transitions of atomic Cu^-.[27]

To produce the oxalic acid dimer anions, oxalic acid was placed in a small oven (~40 °C) attached to the front of a pulsed (10 Hz) valve (General Valve Series 9), where helium (~30 psi) was expanded over the sample in a high vacuum chamber (10^{-6} Torr). Just outside the orifice of the oven, low-energy electrons were produced by laser/photoemission from a pulsed Nd:YAG laser beam (10 Hz, 532 nm) striking a translating, rotating, copper rod (6.35 mm diameter). Negatively charged anions were then pulse-extracted into the spectrometer prior to mass selection and photodetachment.

Results

In Fig. 1 we listed only these conformers of the neutral (**N*n***), anionic (**A*n***), deprotonated (**DP*n***), hydrogenated (**H*n***), and protonated (**P*n***) conformers of OA that are critical for the discussion of our results for $(OA)_2^-$. The complete lists of these conformers, and their relative stability, are presented in the ESI,† Fig. S1–S5. The energies of all the moieties listed in Fig. 1 are with respect to **N1**. The data show that the dissociative asymptotes **N1** + **A1** and **H1** + **DP1** differ by only 0.06 eV, and the latter is actually lower (see Fig. 3). It might be a characteristic feature of the OA + OA^- system. Formation of a zwitterionic, but infinitely separated, pair **P1** + **DP1** requires 6.34 eV, but the AEA of **P1** (7.15 eV) brings the **H1** + **DP1** asymptote below the **N1** + **A1** asymptote. It implies that the anionic clusters of oxalic acid are predisposed to intermolecular proton transfer. The AEA of **N1** is 0.72 ± 0.05 eV, based on anion photoelectron data[1] and 0.75 eV, as computed here.

Analogous asymptotes for the neutral and anionic FA dimer are shown in Fig. S6 (ESI†). The first difference between FA and OA is that the monomer of the former does not bind an electron.[1] Moreover, the formation of the zwitterionic pair **P1** + **DP1** requires more energy in $(FA)_2$ than in $(OA)_2$, 7.23 *vs.* 6.34 eV. Quenching **P1** with an excess electron releases less energy in $(FA)_2^-$ than in $(OA)_2^-$, 6.42 *vs.* 7.15 eV. In consequence, the **H1** + **DP1** asymptote in $(FA)_2^-$ is higher than the **N1** + **N1** + **e** asymptote by 0.81 eV. We conclude that the stability of $(FA)_2^-$ hinges on the two-body interaction term $E^{2b}_{HmDPn}(G)$, eqn (7). Indeed, the energies of the neutral and anionic FA dimer are very similar (|AEA| < 20 meV), though they differ in the distribution of protons.[9]

Back to oxalic acid, in Fig. 1 we included not only the global minimum of HOA•, **H1**, but also the stationary points **H5** and **H8**, which may be viewed as building blocks of the most stable anionic dimers, see Fig. 2 and 4. The planar **H5** and **H8** stationary points are not minima and have one and two imaginary frequencies, respectively. **H5** is a transition state that connects two minima, **H1** and **H3**. **H8** collapses into the isomers of **H7** (see Fig. S4 (ESI†) for all the **H*n*** stationary points).

The energies of the most stable neutral and anionic dimers, **ND1** and **AD1**, respectively, with respect to their dissociative asymptotes are illustrated in Fig. 2. Upon the excess electron attachment, the side-to-side **ND1** undergoes intermolecular proton transfer and morphs into **H5DP1**, the sixth most stable

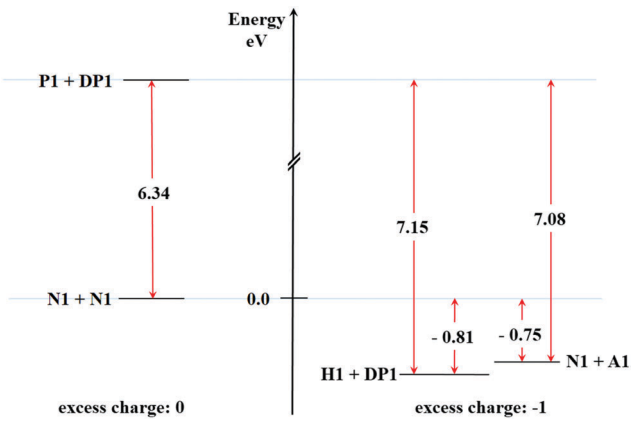

Fig. 3 Relative energies of the dissociative asymptotes for $(OA)_2$ (left) and $(OA)_2^-$ (right). The energy of the **N1** + **N1** asymptote is set to zero.

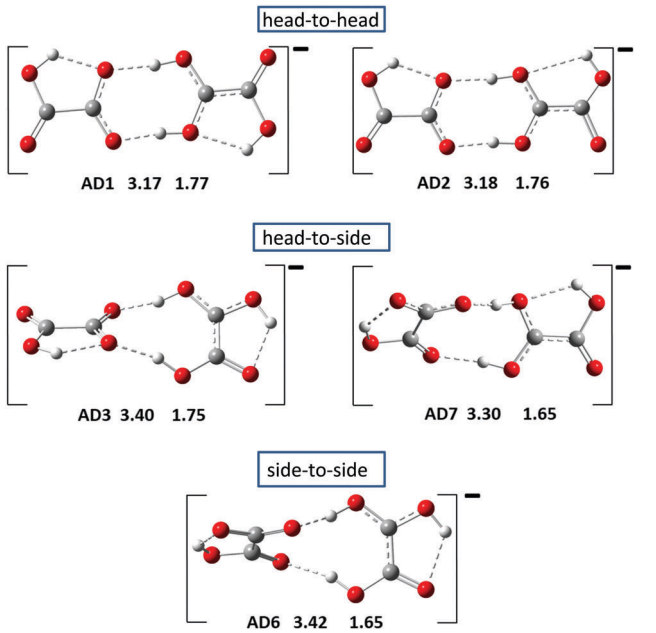

Fig. 4 The most stable isomers of $(OA)_2^-$. The label **AD*n*** is followed by the electron vertical detachment energy and the adiabatic electron affinity with respect to **ND1**. Both energies are in eV.

anionic structure, **AD6**. The most stable anionic dimer **AD1** proves to be **H8DP1**, and it morphs into the head-to-head **ND3** upon the excess electron detachment. We conclude that the most stable anionic and neutral dimers differ qualitatively: the global anionic minimum belongs to the head-to-head family, but the global neutral minimum to the side-to-side family. It is also remarkable how stable these anionic dimers are, with the AEA values exceeding 1.6 eV.

Intermolecular proton transfer is a persistent feature among low-energy isomers of $(OA)_2^-$, but we can still identify three groups that can be traced back to the three most stable groups of neutral dimers:[6] head-to-head, head-to-side, and side-to-side. The representatives of these families are illustrated in Fig. 4. These are: **AD1** and **AD2** (head-to-head), **AD3** and **AD7** (head-to-side), and **AD6** (side-to-side), and their stability with respect to **H1** + **DP1** is detailed in Table 1 (the seven most stable anionic isomers are characterized in Fig. S7 and Table S1, ESI†). All these isomers of $(OA)_2^-$ can be viewed as a **H*n*** monomer interacting with **DP1**. They are non-planar, with the buckling and twisting localized on the **H*n*** unit (for the detailed structural information see Table S2, ESI†). The proton transfer and non-planarity compound to the significant values of VDE, from 3.17 to 3.42 eV. The AEA values presented in Fig. 4 are with respect to **ND1**. They span a narrow range of 0.12 eV (from 1.65 to 1.77 eV).

The relative stability of selected anionic isomers is analysed in Table 1 in terms of one- and two-body terms (see eqn (2)–(7)). These anionic structures involve the deformed HOA$^\bullet$ moieties that resemble the stationary points **H8** and **H5**, which are not minima for the isolated HOA$^\bullet$. The attractive two-body interaction energy plays the dominant role in the overall stability of the anions. The strongest two-body interactions are observed in the head-to-head group, up to −2.27 eV, though they are accompanied by the most repulsive one-body terms, up to 0.88 eV. In the head-to-side group, there are two possible directions of proton transfer: to the monomer that offers its "side" (**AD3**) or its "head" (**AD7**) for hydrogen bonding. The two-body terms are very similar −2.04 and −2.08 eV, respectively, but the penalizing one-body terms render **AD3** more stable than **AD7** by 0.10 eV. Finally, **AD6** is characterized by the weakest two-body term, −1.88 eV, but also the least penalizing one-body terms, 0.61 eV, resulting in a competitive value of the overall stabilization energy. A similar balancing act was observed in the neutral **ND1**.[6]

The photoelectron spectrum of the oxalic acid dimer anion is presented in Fig. 5. The spectrum consists of a broad feature, with an onset of 2.5 eV and spanning to 4.3 eV. The vertical detachment energy (VDE) is assigned to be 3.3 eV, thus in very good agreement with the calculated values.

Discussion

The anion of the oxalic acid dimer has been characterized experimentally, using anion photoelectron spectroscopy, and theoretically, at the CCSD(T) level, with the SCF and MP2-correlation energies extrapolated to the basis set limit.

The first remarkable feature is that the HOA$^\bullet$ + $(OA–H)^-$ dissociative asymptote is lower than the OA + OA^- asymptote by 0.06 eV. In consequence, the most stable anionic structures might be viewed as complexes of a neutral, doublet, hydrogenated moiety HOA$^\bullet$ coordinated to an anionic, singlet, deprotonated moiety $(OA–H)^-$. HOA$^\bullet$ acts as a double proton donor and $(OA–H)^-$ as a double proton acceptor. Thus the excess electron attachment drives intermolecular proton transfer. The low-energy anionic dimers involve the HOA$^\bullet$ moieties more similar to first- and second-order saddle points than to local minima. The calculated AEA values are respectable, in the 1.65–1.77 eV range. Due to intermolecular proton transfer and buckling of the dimer structure, the calculated VDE values are significantly higher and cover the 3.17–3.42 eV range.

The photoelectron spectrum of $(OA)_2^-$ is principally consistent with the calculated characteristics of the anionic dimer. However, the experimental VDE assigned to 3.3 eV is larger than the VDE of the most stable anionic structures **AD1** and **AD2**. The discrepancy might be a manifestation of inaccuracy of theoretical predictions. Another possibility is that the anionic beam is not in thermal equilibrium and it is enriched with **AD6** and **AD3** (or **AD7**). These anions would be formed without additional barrier if the excess electron was attached to the most stable neutral dimers **ND1** and **ND2**, which represent the side-to-side and head-to-side structures, respectively. Indeed, our preliminary explorations of transformation pathways indicate that **AD6** is separated from

Table 1 Total stabilization energy, its components (eqn (1)–(7)), and a correction for the zero-point vibrations for the representative anions of the head-to-head (h-2-h), head-to-side (h-2-s), and side-to-side (s-2-s) groups. All energies are in meV

Type	$(OA)_2^-$	Monomers	$E_{z_n}^{1b-conf}$	$E_{z_n}^{1b-def}(G)$	$E_{z_n}^{1b}(G)$	$E_{X_mY_n}^{2b}$	$E_{X_mY_n}^{stab}$	ΔE_0^{vib}	$E_{X_mY_n}^{stab} + \Delta E_0^{vib}$
h-2-h	AD1	H8	716	138	854	−2267	−1387	0	−1387
		DP1	0	27	27				
	AD2	H8	716	130	846	−2246	−1374	0	−1374
		DP1	0	25	25				
h-2-s	AD3	H5	485	160	644	−2041	−1370	2.	−1367
		DP1	0	27	27				
	AD7	H8	716	66	783	−2084	−1270	5	−1265
		DP1	0	32	32				
s-2-s	AD6	H5	485	99	584	−1882	−1273	4	−1269
		DP1	0	25	25				

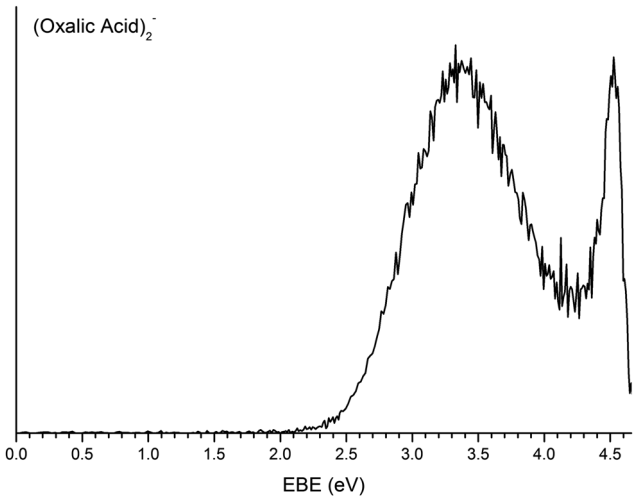

Fig. 5 Photoelectron spectrum of oxalic acid dimer anion.

AD3 by low barriers, less than 47 meV at the MP2/aug-cc-pVDZ level. However, there is a barrier of 409 meV along the **AD3**-to-**AD1** pathway. More extensive analysis of transformation pathways in the neutral and anionic dimer will be presented in our future report.

Is there any effect of dicarboxylic character on the electrophilicity of OA and $(OA)_2$? Here we compare the vertical and adiabatic electron binding energies in $(OA)_n^-$ and $(FA)_n^-$, $n = 1$, 2. The FA monomer does not support a bound valence anionic state but OA^- displays a vertical and adiabatic electron binding energy of 1.08 and 0.72 eV, respectively.[1] Both $(FA)_2^-$ and $(OA)_2^-$ undergo intermolecular proton transfer upon electron attachment, but the VDE is larger for $(OA)_2^-$ by 0.9 eV, as the values for $(FA)_2^-$ are 2.35 eV[9] (computational) and 2.40 eV[10] (experimental). The AEA values for various isomers of $(OA)_2^-$ are substantial, 1.65–1.77 eV, but the result for $(FA)_2^-$ is close to zero ($|AEA| < 20$ meV).[9] These results strongly suggest that the proximity of two carboxylic groups in each OA monomer contributes to the stability of $(OA)_n^-$.

The singly occupied molecular orbitals for one anionic dimer from each group (**AD1**, **AD3**, and **AD6**) are plotted in Fig. 6. Next to each dimer anion **H*m*DP1**, we also show a SOMO of the **H*m***, but at its equilibrium geometry. The striking similarities between the dimer and monomer SOMO's reinforce our interpretation of the anionic dimers in terms of the **H*m*···DP1** complexes. The singly occupied molecular orbital is of π symmetry. It is characterized by a bonding C–C interaction and antibonding C–O interactions. The bonding C–C interaction is possible due to the dicarboxylic character of OA.

We expect that the oxalic acid clusters, due to their significant electrophilicity and experimental accessibility, will become model hydrogen bonded systems for experimental and theoretical studies of proton transfer upon an excess electron attachment.

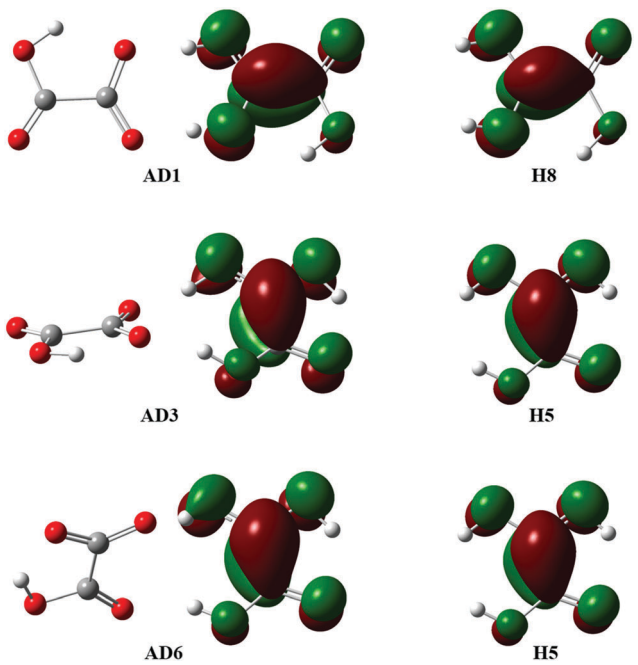

Fig. 6 The isosurfaces of singly occupied molecular orbitals in **AD1**, **AD3**, and **AD6** (left) and the corresponding **H*n*** radicals (right); all species at their equilibrium geometries. The contour values were selected to reproduce 80% of electron density[26] and span a narrow range from 0.051 to 0.054 $a_0^{-3/2}$.

Conflicts of interest

There are no conflicts to declare.

Acknowledgements

Z. G. K. was supported by the fellowship from the University of Botswana (UB). This material is based in part on work supported by the U.S. National Science Foundation under Grant No's. CHE-1360692 and CHE-1664182 (KHB). This work was conducted within the framework of the COST Action CM1301 (CELINA). The research used resources of the National Energy Research Scientific Computing Centre (NERSC), which is supported by the Office of Science of the U.S. Department of Energy under Contract No. DE-AC02-05CH11231.

References

1 A. Buonaugurio, J. Graham, A. Buytendyk, K. H. Bowen, M. R. Ryder, Z. G. Keolopile, M. Haranczyk and M. Gutowski, *J. Chem. Phys.*, 2014, **140**, 221103.
2 J. Nieminen, M. Rasanen and J. Murto, *J. Phys. Chem.*, 1992, **96**, 5303–5308.
3 E. M. S. Maçôas, R. Fausto, M. Pettersson, L. Khriachtchev and M. Räsänen, *J. Phys. Chem. A*, 2000, **104**, 6956–6961.
4 P. D. Godfrey, M. J. Mirabella and R. D. Brown, *J. Phys. Chem. A*, 2000, **104**, 258–264.
5 S. A. Blair and A. J. Thakkar, *Chem. Phys. Lett.*, 2010, **495**, 198–202.
6 Z. G. Keolopile, M. R. Ryder and M. Gutowski, *J. Phys. Chem. A*, 2014, **118**, 7385–7391.
7 G. Buemi, *J. Phys. Org. Chem.*, 2009, **22**, 933–947.

8 J. G. Chang, H. T. Chen, S. C. Xu and M. C. Lin, *J. Phys. Chem. A*, 2007, **111**, 6789–6797.
9 R. A. Bachorz, M. Haranczyk, I. Dabkowska, J. Rak and M. Gutowski, *J. Chem. Phys.*, 2005, **122**, 204304.
10 H. K. Gerardi, A. F. DeBlase, C. M. Leavitt, X. Su, K. D. Jordan, A. B. McCoy and M. A. Johnson, *J. Chem. Phys.*, 2012, **136**, 134318.
11 M. Allan, *Phys. Rev. Lett.*, 2007, **98**, 123201.
12 A. Kumar and M. D. Sevilla, *Chem. Rev.*, 2010, **110**, 7002–7023.
13 C. J. Chang, M. C. Y. Chang, N. H. Damrauer and D. G. Nocera, *Biochim. Biophys. Acta, Bioenerg., 2004*, 1655, 13–28.
14 L. Sanche, *Eur. Phys. J. D*, 2005, **35**, 367–390.
15 J. L. Dempsey, J. R. Winkler and H. B. Gray, *Chem. Rev.*, 2010, **110**, 7024–7039.
16 I. Utke, P. Hoffmann and J. Melngailis, *J. Vac. Sci. Technol., B*, 2008, **26**, 1197–1276.
17 K. E. Riley, M. Pitonak, P. Jurecka and P. Hobza, *Chem. Rev.*, 2010, **110**, 5023–5063.
18 C. Møller and M. S. Plesset, *Phys. Rev.*, 1934, **46**, 618–622.
19 R. A. Kendall, J. Thom, H. Dunning and R. J. Harrison, *J. Chem. Phys.*, 1992, **96**, 6796–6806.
20 R. J. Bartlett and M. Musial, *Rev. Mod. Phys.*, 2007, **79**, 291–352.
21 S. F. Boys and F. Bernardi, *Mol. Phys.*, 1970, **19**, 553–566.
22 S. Simon, M. Duran and J. J. Dannenberg, *J. Chem. Phys.*, 1996, **105**, 11024–11031.
23 M. Gutowski and G. Chalasinski, *J. Chem. Phys.*, 1993, **98**, 5540–5554.
24 M. J. Frisch, G. W. Trucks, H. B. Schlegel, G. E. Scuseria, M. A. Robb, J. R. Cheeseman, G. Scalmani, V. Barone, B. Mennucci, G. A. Petersson, H. Nakatsuji, M. Caricato, X. Li, H. P. Hratchian, A. F. Izmaylov, J. Bloino, G. Zheng, J. L. Sonnenberg, M. Hada, M. Ehara, K. Toyota, R. Fukuda, J. Hasegawa, M. Ishida, T. Nakajima, Y. Honda, O. Kitao, H. Nakai, T. Vreven, J. A. Montgomery Jr., J. E. Peralta, F. Ogliaro, M. Bearpark, J. J. Heyd, E. Brothers, K. N. Kudin, V. N. Staroverov, R. Kobayashi, J. Normand, K. Raghavachari, A. Rendell, J. C. Burant, S. S. Iyengar, J. Tomasi, M. Cossi, N. Rega, J. M. Millam, M. Klene, J. E. Knox, J. B. Cross, V. Bakken, C. Adamo, J. Jaramillo, R. Gomperts, R. E. Stratmann, O. Yazyev, A. J. Austin, R. Cammi, C. Pomelli, J. W. Ochterski, R. L. Martin, K. Morokuma, V. G. Zakrzewski, G. A. Voth, P. Salvador, J. J. Dannenberg, S. Dapprich, A. D. Daniels, Ö. Farkas, J. B. Foresman, J. V. Ortiz, J. Cioslowski and D. J. Fox, Gaussian, Inc., Wallingford CT, 2009.
25 R. Dennington, T. Keith and J. Millam, Semichem Inc., Shawnee Mission, KS, 2009.
26 M. Haranczyk and M. Gutowski, *J. Chem. Theory Comput.*, 2008, **4**, 689–693.
27 J. Ho, K. M. Ervin and W. C. Lineberger, *J. Chem. Phys.*, 1990, **93**, 6987–7002.

